On-Line State and Parameter Identification of Positive Photoresist Development

The development phase of the optical photolithography process has long been considered the most crucial, as it is the final image-forming step. Process monitoring methods have focused primarily on end point detection and have not used other inferable on-line information. This paper examines the use of mathematical models in conjunction with on-line development penetration data to determine process changes. An on-line sequential parameter identification scheme is used to calculate a current rate parameter value for the development model, and a Kalman filter is used to reduce erroneous observations caused by measurement noise. A powerful development monitor system results from the combination of real-time data, and on-line parameter and state estimation theory.

Thomas A. Carroll
W. Fred Ramirez
Department of Chemical Engineering
University of Colorado
Boulder, CO 80309

Introduction

Positive optical photoresists are used in semiconductor and printed circuit board applications to mask selected areas from chemical or physical changes. A substrate is cleaned, dried, and coated with a liquid photoresist solution. The solution consists of solvent, photoactive compound and a resin. The solvent is driven off by baking the coating, leaving behind a film that is typically 1–20 μm thick. A patterned glass photomask is aligned over the substrate, and the resist is exposed by a light in the wavelength range of 350–450 nm (monochromatic or polychromatic). The areas exposed convert from a diazonapthoquinone to a carboxylic acid, which may later be developed using a base. The resist film may be subjected to a post-exposure bake, which alleviates a standing wave problem created by the combination of light diffraction caused by the photomask slits and the reflection of light back from the substrate. The resulting film is developed and rinsed, leaving behind the desired pattern. After a hard bake, the required process is performed on the substrate. Finally, the resist film is completely removed using a general solvent such as acetone.

The development phase of the positive optical photoresist process has been monitored using interferometric techniques described by Willson (1983), Lauchlan et al. (1985), and Novembre et al. (1989). During development, a collimated beam of nonexposing light is allowed to shine on a substrate coated with a film of exposed photoresist. The light reflections from the resist/developer interface and the substrate are collected and read by a photodiode. The resulting signal, sinusoidal in nature, indicates the constructive and destructive interferences caused by the two reflections, thus allowing calculation of both the rate of development and the resist thickness of the developing region. Sautter et al. (1989) expanded the work of Lauchlan et al. to use the end point detector to monitor line width variation, development uniformity, and certain process failures.

Mack (1983, 1985) has presented a mathematical model which describes the development process. This model, combined with the available process measurement, can be used to estimate the depth of penetration of the developer into the resist film and to update model parameters. By using on-line parameter and state identification, process parameters can be adjusted from one substrate to the next automatically.

This paper describes state and parameter identification for a spray development process using a modified APT spray-spin developer. Simulations and experimental data presented show the power of combining model and real-time data in obtaining a useful endpoint detector which not only provides a means of development control, but also a process parameter monitoring scheme.

System and State Definition

The contact/proximity printing process for positive optical resists has several steps, of which exposure and development are the most important in constructing a process model. Measure-

Correspondence concerning this paper should be addressed to W. F. Ramirez.

ments are also required if any model modification is to be implemented on-line during process operation. Development progress can be monitored by striking the resist-coated substrate with a collimated beam of nonexposing light. Interference fringes, resulting from the changes in reflection from the resist/developer interface with respect to reflection from the substrate, provide resist thickness data and rate of dissolution during development (Lauchlan et al., 1985).

Figure 1 shows the simplified cross-section of an exposed line of resist, thickness z_0. Let z represent the depth of penetration of development into the resist film and y be the distance from the center of the line. We desire to develop the resist until a width L is cleared at $z = z_0$. Mack (1985, 1987) has derived a development model which combines the chemistry of dissolution and the mass transfer rate of developer from the bulk to the resist surface. The development rate, expressed as length per time penetration, is given by

$$r = \left\{ k_{\min} + k_D \frac{[1 - M(y,z)]^n}{a + [1 - M(y,z)]^n} \right\} \cdot [1 - (1 - r_0) \exp(-4z/z_t)]\, u(t), \quad (1)$$

where r is the rate of dissolution, $M(y, z)$ is the relative photoactive compound concentration after exposure, $u(t)$ is the control effort expressed as developer concentration, r_0 is the surface development rate relative to the bulk rate, y is the distance from the line width center, z is the depth of penetration into the resist, z_t is the characteristic film depth where surface effects no longer play a significant role in development, $k_{\min}$ is the minimum development rate constant, k_D is the mass transfer coefficient, n is the order of the kinetics of dissolution, and a is a constant given by

$$a = k_D k_R m_0^n, \quad (2)$$

where m_0 is the PAC concentration before exposure and k_R is the reaction rate constant for dissolution. $M(y, z)$ is calculated from PROLITH (Mack, 1985) for given exposure parameters appropriate to the resist and the film's prebake time.

The only available on-line process measurement is the depth of penetration of developer into the resist film. During exposure, light diffraction and reflections from the substrate cause the resist in the line to be exposed unevenly. Thus, the measurement represents only the development of the central region of the line. Once development has penetrated to the substrate in this region ("breakthrough"), real-time data are no longer available.

For on-line processing, it is important to make as many simplifications to the model as possible without removing too much information about the actual physical process. The following assumptions, therefore, were made: 1. the line is symmetric about the $y = 0$ line and 2. development proceeds in the z-direction only. Assumption 2 is not strictly true, but is a reasonable approximation in the breakthrough region.

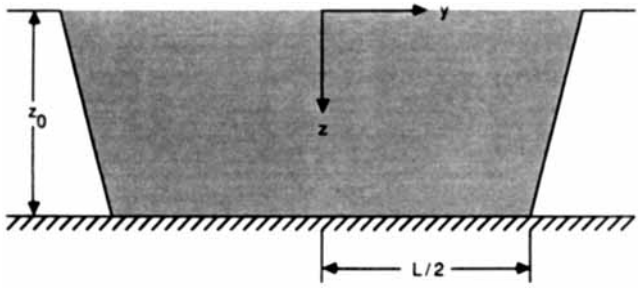

Figure 1. Resist cross-section.

It is convenient to define a set of depths of penetration z_i at given distances y_i from the center of the line width. The states z_i are defined as a vector $\boldsymbol{x}$, which consists of depths z_i from $y = 0$ to $y = L/2$ and beyond. The states of interest are in the breakthrough region only. The rate of dissolution at a given y_i is then

$$r_i = \frac{dz_i}{dt}. \quad (3)$$

The state dynamics in the breakthrough region are given by

$$\frac{dz_i}{dt} = \left[k_{\min} + k_D \frac{(1 - M_i)^n}{a + (1 - M_i)^n} \right] \cdot \left[1 - (1 - r_0) \exp\left(-\frac{4z_i}{z_t} \right) \right] u, \quad (4)$$

where M_i is the value of PAC concentration evaluated as a function of state z_i, and the subscript i denotes all states inside the line width ($i = 1, \ldots, m$). Note that each state equation is independent of the other.

State Identification

Kalman filtering (Sage and White, 1977) is used to balance the mathematical model of a process and available process measurements to produce an optimal state estimate. The process is assumed to have a model given by

$$\boldsymbol{x}_{k+1} = \boldsymbol{\Phi}_k(\Delta t)\boldsymbol{x}_k + \boldsymbol{w}_k, \quad (5)$$

where $\boldsymbol{\Phi}$ is the state transition matrix and $\boldsymbol{w}$ is the uncertainty related to white Gaussian noise, with expected value $E(\boldsymbol{w}) = \boldsymbol{0}$ and covariance $E(\boldsymbol{w}\boldsymbol{w}^T) = \boldsymbol{Q}$. The measurements are related to the states by

$$y_k = \boldsymbol{H}\boldsymbol{x}_k + v_k, \quad (6)$$

where $\boldsymbol{H}$ is the measurement matrix and v is the measurement noise, with expected value $E(v) = 0$ and covariance $E(v^2) = R$. Since only one measurement is available, y_k and R are scalars.

The estimated states, $\hat{\boldsymbol{x}}$, which are used to determine the control status of the development system, are calculated from

$$\hat{\boldsymbol{x}}_k = \bar{\boldsymbol{x}}_k + \boldsymbol{K}_k(y_k - \boldsymbol{H}\bar{\boldsymbol{x}}_k), \quad (7)$$

where the Kalman filter gain, $\boldsymbol{K}$, is recursively determined using

$$\boldsymbol{K}_k = \boldsymbol{P}_k\boldsymbol{H}^T\boldsymbol{R}^{-1} \quad (8)$$

$$\boldsymbol{P}_k = \boldsymbol{M}_k - \boldsymbol{M}_k\boldsymbol{H}^T(\boldsymbol{H}\boldsymbol{M}_k\boldsymbol{H}^T + \boldsymbol{R})^{-1}\boldsymbol{H}\boldsymbol{M}_k \quad (9)$$

$$\boldsymbol{M}_{k+1} = \boldsymbol{\Phi}_k\boldsymbol{P}_k\boldsymbol{\Phi}_k^T + \boldsymbol{Q}. \quad (10)$$

The state transition matrix, $\boldsymbol{\Phi}_k$, is given by the linear approximation

$$\boldsymbol{\Phi}_k = \boldsymbol{I} + (\partial \boldsymbol{f}_k^T/\partial \boldsymbol{x})\Delta t, \quad (11)$$

where

$$f_k = dx_k/dt. \tag{12}$$

The expected value of the states, $\bar{x}$, is determined from the previous estimate using

$$\bar{x}_k = \hat{x}_{k-1} + f_{k-1}(\hat{x}_{k-1})\Delta t. \tag{13}$$

The initial conditions for the states $\hat{x}(0)$, and the state covariance matrix $P(0)$ for the discrete case are

$$\hat{x}(0) = \hat{x}_0 \tag{14}$$

$$P(0) = P_0 = E[(x_0 - \bar{x}_0)(x_0 - \bar{x}_0)^T]. \tag{15}$$

The maxima and minima in the interference wave form, described previously, yield depth measurements given by

$$\Delta z = \lambda/4n_r, \tag{16}$$

where n_r is the average refractive index of the film and λ is the wave length of light. The measurement is thus given by

$$y_k = \frac{(k-1)\lambda}{4n_r} \tag{17}$$

where k represents each interference fringe during development.

For this situation, not all states are observable. The measurement matrix must be split into two sections:

$$H = (1/q)[H_1|H_2] \tag{18}$$

$$H_1 = [1\ 1 \ldots 1] \tag{19}$$

$$H_2 = [0\ 0 \ldots 0]. \tag{20}$$

H_1 is a $q \times 1$ matrix (q being the number of states in the breakthrough region) and H_2 a $(m - q) \times 1$ matrix.

If Φ_k is nearly constant during the process, a steady-state gain matrix K_{ss} can be used in place of the updating procedure of Eqs. 8–11 in order to save several minutes of computational time. The time savings are extremely important in light of the small process time, on the order of one minute. Since endpoint detection is desired, the values of the states are most important around the breakthrough time.

The useful information from the measurements is limited to the time from development startup to breakthrough in the film. Only the q states defined in this limited area are observable. This implies that the Kalman filter algorithm is useful only to optimally identify these states and is useful only until breakthrough occurs. The remaining states can only be estimated using the mathematical model. Since the model prediction is a function of the model parameters, it is useful also to identify, on-line, actual model parameters during the time that data are available.

Parameter Identification

Ljung and Soderstrom (1983) discuss several recursive identification techniques by which model parameters can be updated either on- or off-line. Process variations prior to development may cause significant deviations in a resist line thickness which are evident only after development. By using on-line parameter identification we can finetune the process model by the time breakthrough occurs. A simplified development model was used for this application,

$$\frac{dz_i}{dt} = \left[k_{\min} + k_D \frac{(1 - M_i)^n}{a + (1 - M_i)^n}\right] u(t), \tag{21}$$

where the surface induction effect described by Eq. 4 has been neglected. It is not important to know the specific model dynamics at the surface since data are available until breakthrough. If we let

$$u(t) = Du_1(t), \tag{22}$$

where $u_1 = 1$ when developer fluid is dispensed and 0 when no development takes place, and D is the bulk concentration of active developer in the spray. Equation 21 can be recast as

$$\frac{dz_i}{dt} = k_1\left[k_2 + \frac{(1 - M_i)^n}{a + (1 - M_i)^n}\right] u_1(t), \tag{23}$$

where

$$k_1 = Dk_D \tag{24}$$

and

$$k_2 = k_{\min}/k_D. \tag{25}$$

The parameters k_1, k_2, a and n are calculated from off-line experimental results and used as a first approximation for the on-line identification.

Parameter and state identification can be combined (Ramirez, 1987) using the steady-state Kalman filter gain. Let θ represent the vector of parameters to be identified. The prediction model is of the form

$$\bar{x}_k(\theta) = \hat{x}_{k-1}(\theta) + f_{k-1}(\hat{x}_{k-1}, \theta)\Delta t \tag{26}$$

with the optimal estimate

$$\hat{x}_k(\theta) = \bar{x}_k(\theta) + K_k[y_k - H\hat{x}_k(\theta)] \tag{27}$$

and a linear measurement model is given by

$$\hat{y}_k(t|\theta) = H\hat{x}_k(\theta). \tag{28}$$

The parameters are identified by comparing measured data with the states predicted from the model by the following recursive algorithm (Ramirez, 1987):

$$\hat{x}_k = (I - K_{ss}H)[\hat{x}_{k-1} + \Delta t f_{k-1}(\hat{x}_{k-1})] + K_{ss}y_k \tag{29}$$

$$\hat{\theta}_k = \hat{\theta}_{k-1} + L_k\epsilon_k \tag{30}$$

$$\epsilon_k = y_k - H\hat{x}_k(\theta_{k-1}) \tag{31}$$

$$L_k = P_{k-1}\psi_k/S_k \tag{32}$$

$$S_k = \psi_k^T P_{k-1}\psi_k + \lambda_k\hat{\Lambda}_k \tag{33}$$

$$\hat{\Lambda}_k = \hat{\Lambda}_{k-1} + \gamma_k(\epsilon_k^2 - \hat{\Lambda}_{k-1}) \tag{34}$$

Table 1. Exposure and Development Parameters Used in Simulation

PAC Absorbance, A	0.86 μm^{-1}
Inert Absorbance, B	0.07 μm^{-1}
Exposure reaction rate constant, C	0.014 cm^2/mJ
Line Width, L	2.0 μm
Resist Thickness, z_0	2.2 μM
Exposure Dosage	1,500 mJ/cm^2
a	0.01353
n	5.0
$k_{min}u$	0.0005 $\mu m/s$
$k_D u$	0.1 $\mu m/s$
r_0	0.755
z_t	0.4 μm
Light Source	632.8 nm
n_r	1.68

$$\gamma_k = \gamma_{k-1}/(\gamma_{k-1} - \lambda_k) \tag{35}$$

$$\psi_k^T = HW_k \tag{36}$$

$$W_k = F_k W_{k-1} + \overline{M}_k \tag{37}$$

$$\overline{M}_k = (I - K_{ss}H)(\partial f_{k-1}^T/\partial\theta)\Delta t \tag{38}$$

$$F_k = (I - K_{ss}H)\Phi_k(\Delta t, \theta_{k-1}) \tag{39}$$

$$P_k = [P_{k-1} - L_k S_k L_k^T]/\lambda_k. \tag{40}$$

Note that the estimated state is updated from the nonlinear model given by Eqs. 12 and 23. The gradient matrix $\overline{M}$ (Eq. 38) is also calculated using the nonlinear model for a more accurate parameter identification.

The initial conditions are

$$W_0 = 0 \tag{41}$$

$$\hat{\Lambda}_0 = E(\epsilon_0^2) \tag{42}$$

$$\hat{\theta}(0) = \hat{\theta}_0 \tag{43}$$

$$P(0) = P_0 \tag{44}$$

$$\lambda_k(0) = \lambda_0. \tag{45}$$

If the forgetting factor, λ_k, is assumed constant, then γ must also be constant (Eq. 35).

Table 2. Kalman Filter Parameters

Measurement Matrix

$$H = 0.125\,[1\,1\,1\,1\,1\,1\,1\,1\,0\,0\,0\,0\,0]$$

Measurement Covariance

$$r = 0.04\ \mu m^2$$

Model Covariance Matrix

$$Q_{diag} = 0.04\,[1\,1\,1\,1\,1\,1\,1\,1\,1\,4\,4\,4\,4]\ \mu m^2$$

Initial State Covariance Matrix

$$P(0)_{diag} = 2.2\,[1\,1\,1\,1\,1\,1\,1\,1\,0\,0\,0\,0\,0]\ \mu m^2$$

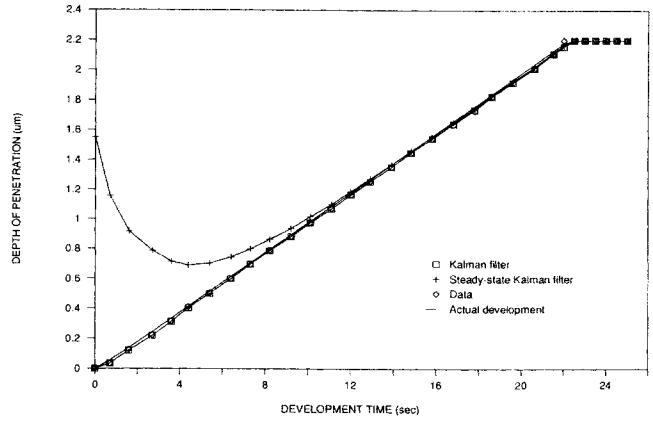

Figure 2. Kalman filter for AZ1350 development simulation.

Simulation

State and parameter identification is simulated for a typical exposed line of AZ1350J photoresist using the process parameters shown in Table 1. Contact exposure is simulated using a typical diffraction distribution generated by PROLITH using parameters taken from the literature (Dill et al., 1975). Values for $M(x_i)$ are determined and stored in memory. The development parameters, shown in Table 1, were obtained from Mack (1987). The light source is assumed to be a He-Ne laser.

The measurements, given as depth of penetration, are simulated using Eq. 1 as the actual system. The development equation is solved to obtain the "true" response to the given inputs and parameters. Using Eqs. 16 and 17, the times at which the interference fringe extrema occur may be computed. An exponentially decaying sinusoid is fit to the extrema, and random noise is introduced to the sinusoid to simulate a real data acquisition system. The resulting wave form is used to test both the state and parameter identification algorithms.

State estimation

The parameters used to evaluate the Kalman filter and state estimates are given in Table 2. The worst case deviation of the normalized depth is assumed to be $\pm 0.2\ \mu m$ for observable states and $\pm 0.4\ \mu m$ for all others. The measurement is assumed to deviate $\pm 0.2\ \mu m$, which is much worse than the actual filtered signal. These severe penalties are used to illustrate the usefulness of Kalman filtering.

Figure 2 shows the simulated estimation of the state defined at the line width center. The simulated data differ from the actual system response because of the presence of noise in the data. Each time an extremum in the interference fringe response

Table 3. Parameter/State Estimation Parameters for Simulation

$k_1 = 0.101\ \mu m/s$; $k_2 = 0.00493$
Covariance of Model Uncertainty: $P_0 = 0.1\ \mu m^2/s^2$
Local Error Covariance: $\hat{\Lambda}_0 = 0.1\ \mu m^2$
Forgetting Factor: $\lambda_k = 0.9$
Initial Parameter Estimate
Case 1: $\hat{\theta}_0 = 0.101\ \mu m/s$
Case 2: $\hat{\theta}_0 = 0.0508\ \mu m/s$

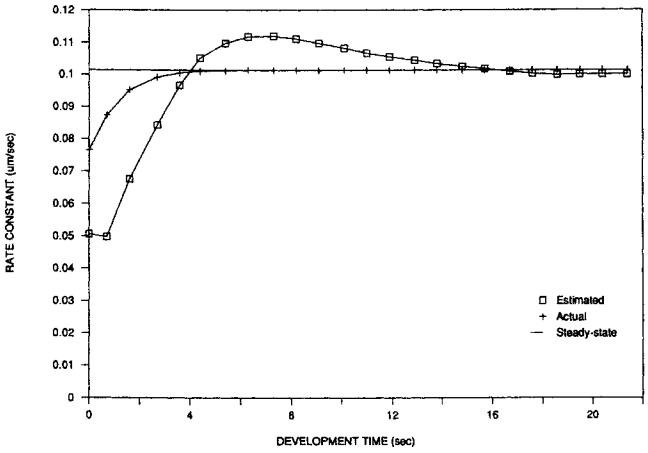

Figure 3. Rate constant for AZ1350 development simulation.

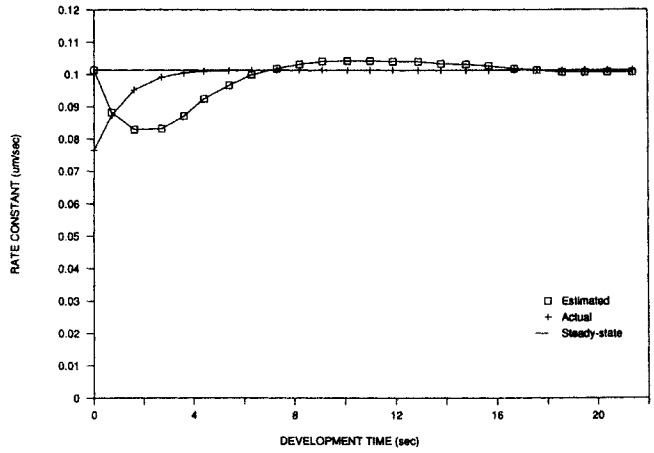

Figure 5. Rate constant for AZ1350 development simulation, case 2.

is detected, the Kalman filter and state are updated using the algorithm in Eqs. 7–13. Figure 2 illustrates three cases:

1. A continuously updated Kalman filter, which assumes an initial worst-case estimate of the depth at $z_i = 2.2\ \mu m$
2. A steady-state Kalman filter, also assuming $z_i = 2.2\ \mu m$ initially
3. The "actual" development assuming $z_i = 0$

The optimum filter, case 1, tracks very closely to actual state value, despite the assumption that the model's "expected" initial depth is 2.2 μm. This occurs because the Kalman filter gain is initially very large, due to the large value of $P(0)$. The dynamic filter gain is in fact so large that a considerable undershoot would occur if constraints on z were not imposed. The states must be constrained in such a way that $0 \le z \le z_0$, which insures proper operation of the algorithm and a proper physical description of the phenomenon. The steady-state filter is much slower than the dynamic filter in correcting the discrepancy between measurement and model since the steady-state gain is two orders of magnitude less than the initial dynamic gain. However, the filter with the steady-state gain tracks well at the crucial time when breakthrough occurs, even for this worst-case scenario.

Parameter estimation

Table 3 shows the parameters used in a combined parameter and state estimation simulation. Parameter k_1 from Eqs. 23 and 24 is to be identified on-line. The vector θ is simply a scalar in this case, k_1. Figure 3 indicates the variation of k_1 as the development proceeds, with an initial estimate of the parameter which is half its actual final value. The actual rate parameter value, $k_{1,a}$, is calculated using

$$k_{1,a} = k_1\left[1 - (1 - r_0)\exp\left(-\frac{4z_i}{z_t}\right)\right]. \qquad (46)$$

Rate parameter $k_{1,a}$ is shown to illustrate the surface induction effect. Note that the estimated parameter, k_1, tracks beyond the final rate parameter value in order to compensate for the initial low guess. The state response, shown in Figure 4, is initially sluggish because the model parameter has not attained the value that is true to the actual system.

The simulation is repeated in Figures 5 and 6 using an initial model parameter value which is close to its final value. Since the initial guess is greater than the actual system parameter, the model parameter undershoots to compensate, causing a sluggish

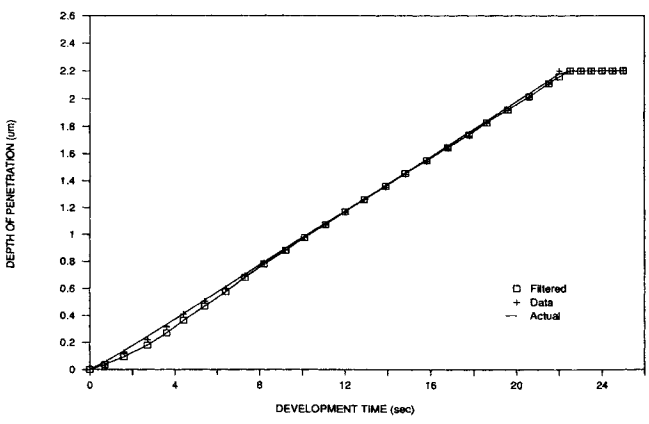

Figure 4. Progress of development for AZ1350 simulation.

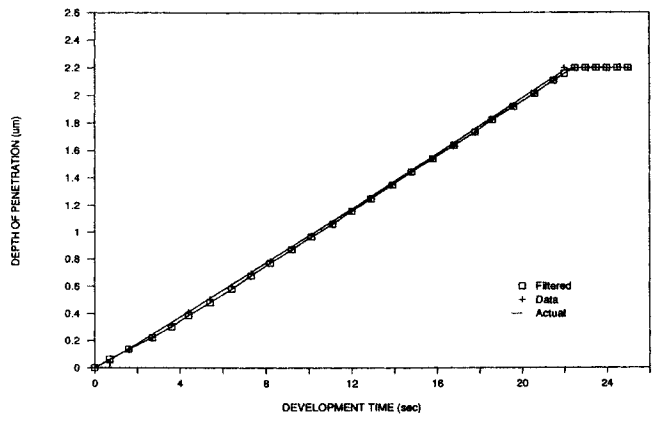

Figure 6. Progress of development for AZ1350 simulation, case 2.

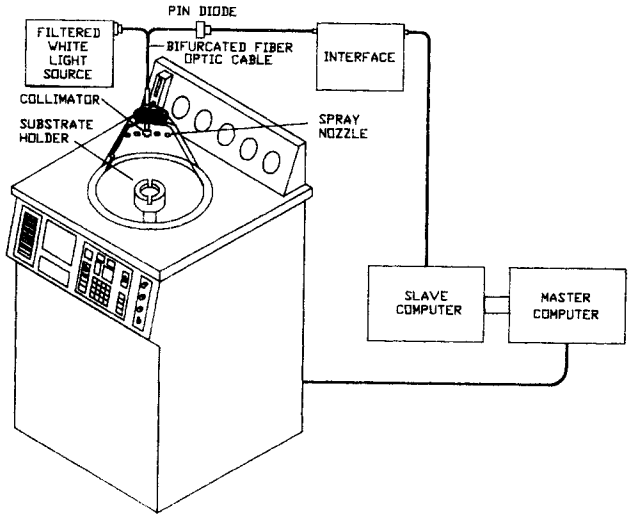

Figure 7. Spray developer and data acquisition system.

response in the states early in the process. As the process nears completion, the actual and estimated parameters at track closely.

Experimental Results

Figure 7 shows the spray developer configuration used to process samples. It is similar to a system used to control resist development on photomask substrates (Novembre et al., 1989). A spray-spin developer, manufactured by APT, was modified to accept commands from a PC-AT, the "master" computer. A bifurcated fiber optic cable carries filtered light from a halogen source and aims it at a developing substrate. The reflections from the substrate are read by a silicon photodiode, prefiltered with an analog amplifier and digitally filtered by an 8088-based PC, the "slave" computer. The slave system calculates the time between interference fringes and sends an interrupt to the master when each new fringe is confirmed. The parameters and states are updated using the algorithm shown in Eqs. 29–45.

Table 4. AZ4330 Parameters Used in Experiments

Development parameters

$a = 0.0636$	$n = 4.77$
$k_1 = 0.102 \mu m/s$	$k_2 = 0.216$
$P_0 = 0.1\ \mu m^2/s^2$	$\hat{\Lambda}_0 = 0.1\ \mu m^2$
$\lambda_k = 0.9$	$\hat{\theta}_0 = 0.102\ \mu m/s$

Exposure Paramters

Wave Length (nm)	A (μm^{-1})	B (μm^{-1})	C (cm^2/mJ)	Fraction of Total Light
365.0	0.468	0.0850	0.0103	0.255
404.7	0.470	0.0310	0.0162	0.203
435.8	0.306	0.0273	0.0085	0.542

$n_r = 1.57$ — Substrate Index $= 2.30 + j3.96$
Dose $= 206.7\ mJ/cm^2$ — $z_o = 4.2\ \mu m$
Line Width $= 5\ \mu m$ — Prebake Time $= 30$ min

Steady-State Kalman Filter Gain Matrix

$$K_{ss}^T = 0.296\ [1\ 1\ 1\ 1\ 1\ 1\ 1\ 1\ 0\ 0\ 0\ 0\ 0]$$

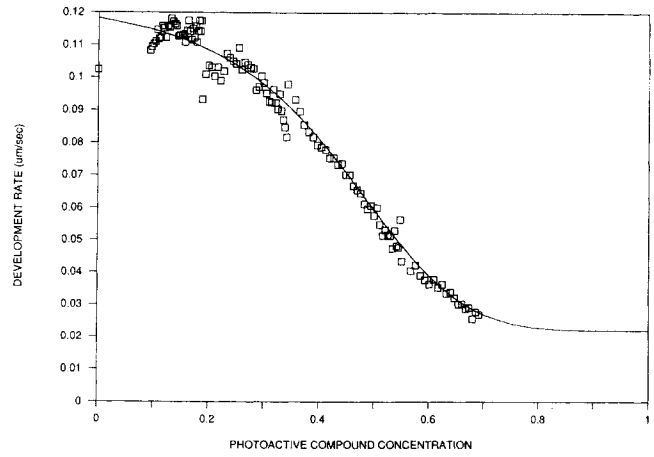

Figure 8. Development rate model fit to AZ4330 resist data.

The substrates were coated with 4.2 μm of AZ4330 resist, exposed by a Canon proximity printer with an energy dose of 206.7 mJ/cm^2. The exposed area is roughly 90%, and the lines are approximately 5 μm wide. The exposure parameters shown in Table 4 were determined using Dill's model and experimental

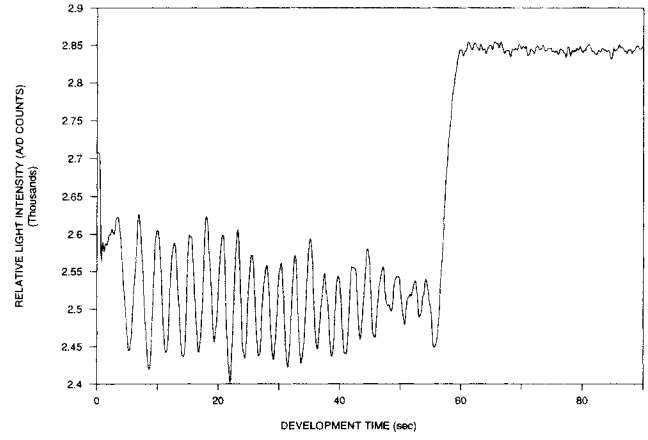

Figure 9. Fringe data for AZ4330 development.

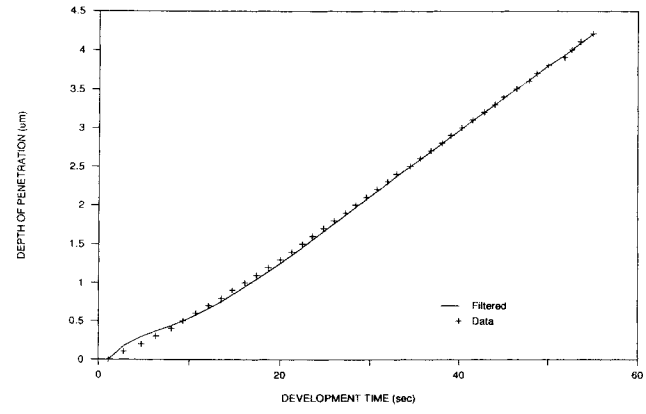

Figure 10. State identification for AZ4330 development.

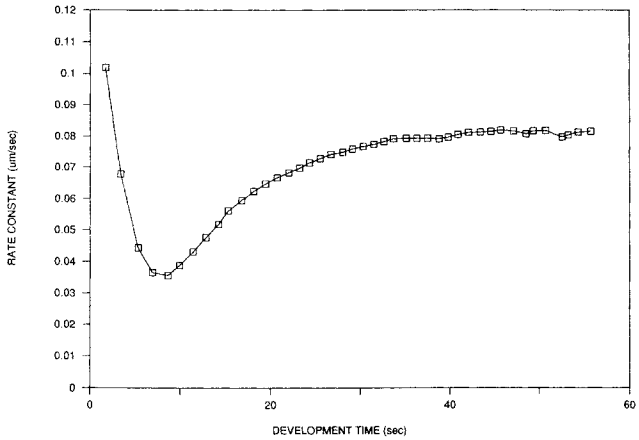

Figure 11. Rate constant for AZ4330 development.

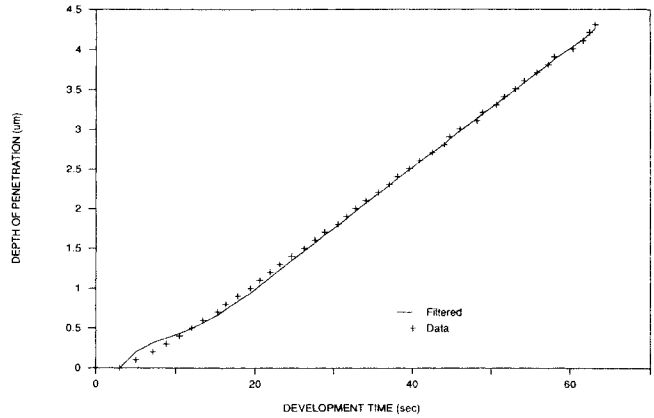

Figure 13. State identification for "noisy" AZ4330 development.

technique, described elsewhere (1975). An approximate photoactive compound (PAC) concentration distribution of the central region is also calculated from Dill's model.

The development parameters used for the Kalman filter are also shown in Table 4. These were obtained by giving a number of substrates blanket exposures at several different dosages and observing the development rate. The development rate as a function of PAC concentration and the model fit are shown in Figure 8.

Figure 9 shows a monitored development experiment. The interference filter used in the fiber optic source is 630 nm with a bandwidth of 10 nm. Using Eq. 16, the number of interference fringes and the development rate may be calculated. The Kalman filter parameters, unchanged from the simulation, are used to calculate the steady-state Kalman filter gain matrix. The combined parameter and state identifier calculates the depth of penetration of the development, as shown in Figure 10. The filtered state initially shows a faster development than the data indicates, but after the transients have died away, the response tracks closely with the raw data.

Figure 11 shows the updated parameter, which represents the development rate constant. Note that the parameter value dips initially, indicating the surface induction effect. The parameter becomes relatively constant as the development nears breakthrough.

There exists a possibility that the computer algorithm which counts interference fringes may fail to recognize a true fringe or count an extra fringe in a noisy peak. These occurrences may be defined as measurement noise. The steady-state Kalman filter is used to help reduce glitches caused by this noise. Figures 12 through 14 show a case where some of the sinusoid peaks are obscured by noise. The actual film depth cannot be accurately measured in this circumstance, since the number of fringes counted by software exceeds the number of fringes which are visually noticeable. The development rate may be approximated, however, and the model parameters estimated on-line. The software has no trouble identifying the endpoint, so the process may still be monitored despite the substantial noise problem. It is also interesting to note that the latter experiment is run at a lower temperature. The parameter identification scheme accordingly yields a lower rate constant for the run, as shown in Figure 14. Transient startup conditions are not concerns either, since the parameter identifier can calculate the proper rate while the Kalman filter can adequately monitor development progress.

Conclusions

An on-line state and parameter estimator has been formulated theoretically, and programmed and tested for a spray

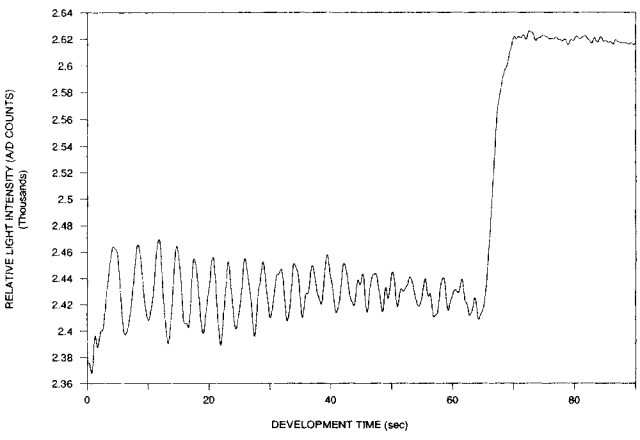

Figure 12. Noisy fringe data for AZ4330 development.

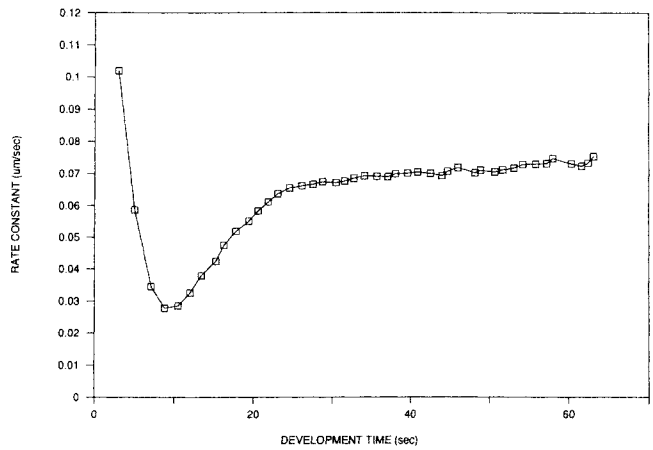

Figure 14. Rate constant for "noisy" AZ4330 development.

development system for positive optical photoresists. It makes use of not only the end-point information, but also the interference fringes generated during development. This information is used to update a process model, which in turn may be used to control line width more consistently. Kalman filtering was used to balance noisy data with expected process observations. The use of the parameter identifier also illustrates the effects of surface induction described in previous work.

Acknowledgement

The authors gratefully acknowledge the financial support of the Storage Technology Corporation.

Notation

a = constant, $k_D / k_R m_0^n$, dimensionless
D = bulk developer concentration, mol/L
$E(*)$ = expected value
$\boldsymbol{F}$ = linear discrete model matrix
f = system equation vector
f_ℓ = single member of system vector
$\boldsymbol{H}$ = measurement matrix
i = subscript denoting states inside line width
$\boldsymbol{K}$ = Kalman filter gain matrix
$\boldsymbol{K}_{ss}$ = steady-state Kalman filter gain matrix
k = discrete time step
k_1 = estimated development rate parameter, s^{-1}
$k_{1,a}$ = actual development rate parameter, s^{-1}
k_2 = development parameter, dimensionless
k_D = mass transfer coefficient, $\mu m \cdot L/mol \cdot s$
k_{min} = reaction rate constant for unexposed resist, $\mu m \cdot L/mol \cdot s$
k_R = reaction rate constant, $\mu m \cdot L/mol \cdot s$
ℓ = general subscript
$\boldsymbol{L}$ = gain matrix
L = line width, μm
m = total number of states inside line width
m_0 = preexposure photoactive compound concentration, mol/L
M = relative post-exposure PAC concentration, dimensionless
$\boldsymbol{M}$ = intermediate result matrix
$\overline{\boldsymbol{M}}$ = gradient matrix
n = dissolution reaction order, dimensionless
n_r = average refractive index of photoresist, dimensionless
$\boldsymbol{P}$ = state covariance matrix
$\boldsymbol{P}_0$ = initial state covariance matrix
$\boldsymbol{Q}$ = model covariance
r = rate of dissolution, $\mu m/s$
$R, \boldsymbol{R}$ = measurement covariance
r_0 = surface development relative to bulk rate, dimensionless
t = time
$u(t)$ = control effort, mol/L
$u_1(t)$ = scaled control effort
$v, \boldsymbol{v}$ = measurement noise vector (scalar)
$\boldsymbol{W}$ = recursive gradient model matrix
$\boldsymbol{w}$ = process noise vector
$\boldsymbol{x}$ = state vector, dimensionless
$\bar{\boldsymbol{x}}$ = expected value of states
$\hat{\boldsymbol{x}}$ = estimated states
$\boldsymbol{x}_0$ = initial states
y = distance from line width center, μm
$y, \boldsymbol{y}$ = measurement vector (scalar)
z = depth of penetration, μm
z_0 = photoresist film thickness before exposure, μm
z_l = depth of penetration at a given distance from line width
z_t = characteristic depth where surface effect is negligible, μm

Greak letters

γ = scalar gain
ϵ = error between data and measurement model
$\theta, \hat{\theta}$ = parameter vector
Λ = covariance of the error between data and measurement model
λ = light wavelength, nm
λ_k = forgetting factor
Φ = transition matrix
ψ = gradient matrix

Literature Cited

Dill, F. H., W. P. Hornberger, P. S. Hauge, and J. M. Shaw, "Characterization of Positive Photoresist," *IEEE Trans. Elect. Dev.*, **ED-22** (7), 445 (1975).

Lauchlan, L., K. Sautter, T. Batchelder, and J. Irwin, "In-line Automatic Photoresist Process Control," *Proc. SPIE, Advances in Resist Technology and Processing II*, **539**, 227 (1985).

Ljung, L., and T. Soderstrom, *Theory and Practice of Recursive Identification*, MIT Press, Cambridge, MA (1983).

Mack, C. A., "Development of Positive Photoresists," *J. Electrochem. Soc.*, **134**(1), 148 (1987).

———, "PROLITH: a Comprehensive Optical Lithography Model," *Proc. SPIE (Optical Microlithography IV)*, **538**, 207 (1985).

Novembre, A. E., W. T. Tang, and P. Hsieh, "An In Situ Interferometric Analysis of Resist Development on Photomask Substrates," *Proc. SPIE (Integrated Circuit Metrology, Inspection, and Process Control III)*, **1087**, 460 (1989).

Ramirez, W. F., "Optimal State and Parameter Identification. An Application to Batch Fermentation," *Chem. Eng. Sci.*, **42**(11), 2749 (1987).

Sage, A. P., and C. C. White, *Optimum Systems Control*, 2nd ed., Prentice-Hall Inc., Englewood Cliffs, NJ (1977).

Sautter, K. M., M. Ha, and T. Batchelder, "Development Process Control Utilizing an End Point Monitor," *Proc. SPIE (Integrated Circuit Metrology, Inspection, and Process Control III)*, **1087**, 312 (1989).

Willson, C. G., "Organic Resist Materials—Theory and Chemistry," *Introduction to Microlithography*, ACS Symp. Ser., **219**, 100, L. F. Thompson, C. G. Willson, and M. J. Bowden, eds. (1983).

Manuscript received Jan. 18, 1990, and revision received June 8, 1990.